B spectroscopy and glueball searches with the OPAL detector at LEP

Michael Thiergen[a]
for the OPAL collaboration

[a]Albert-Ludwigs-Universität Freiburg, Fakultät für Physik,
Hermann-Herder-Str. 3, 79104 Freiburg i. Br., Germany

Recent results from OPAL analyses on B meson spectroscopy are reviewed. Measurements are compared with those of other experiments and with theoretical expectations. In addition, a search for the tensor glueball candidate $f_J(2220)$ in hadronic Z^0 decays is presented. No signal is observed in the $K^0_s K^0_s$ final state and an upper limit is placed on the production rate of $f_J(2220) \to K\bar{K}$ in $Z^0 \to q\overline{q}$ decays.

1. B MESON SPECTROSCOPY

1.1. Introduction

Mesons containing one heavy quark Q, $m_Q \gg \Lambda_{QCD}$, provide a good environment for testing QCD. In the heavy quark limit $m_Q \to \infty$, the spin of the heavy quark decouples and the total spin J of the meson as well as the angular momentum of the light component $j_q = L + S_q$ become conserved quantum numbers (Heavy Quark Symmetry, HQS). For each angular momentum L, there is a degenerate doublet with $j_q = L \pm \frac{1}{2}$. For $Q = \bar{b}$ and $L = 0$, we thus obtain the ground states B and B*. For $L = 1$, two doublets corresponding to $j_q = \frac{1}{2}$ and $j_q = \frac{3}{2}$ resemble the lowest-lying orbitally-excited states, collectively labelled[1] B^*_J. The intra-doublet mass splittings scale with Λ^2_{QCD}/m_b in the heavy quark expansion. All bottom ground state mesons except the B^*_c are well established by experiment [1]. Orbitally-excited mesons B^*_J and B^*_{sJ} have been observed by LEP experiments and recently also by CDF. The evidence claimed for radially-excited (2S) B mesons [2,3] is still not confirmed.

At LEP, B mesons are produced in the process $e^+e^- \to Z^0/\gamma^* \to b\bar{b}$. Excited B mesons decay strongly or electromagnetically to the weakly decaying ground states via emission of π, $\pi\pi$, K or γ. The B four-momentum is reconstructed by assigning decay particles to the B meson and discriminating them from fragmentation particles. High resolution silicon micro-vertex detectors provide precise lifetime information and the tagging of $Z^0 \to b\overline{b}$ decays and b hadron reconstruction are achieved using sophisticated algorithms. The range of methods covers fully reconstructed B mesons [4] with good resolution but poor statistics, semi-inclusive [5] to totally inclusive [3,6–8] methods which exploit properties common to all b hadron decay modes. The latter provide high statistics but a moderate direction and energy resolution.

[1]The notation B** is also used for the $L = 1$ states.

1.2. B* mesons

Due to the small mass splitting of $\Delta M(\mathrm{B}^*{-}\mathrm{B}) = 46$ MeV the B* decays predominantly into Bγ. At LEP this results in photon energies of $E_{\gamma,\mathrm{lab}} \leq 800$ MeV. To achieve a good B* mass resolution, only photons which converted in the material of the inner tracking system are combined with inclusively reconstructed B mesons. The B reconstruction is based on lifetime information and kinematics. A decay weight ω_i is assigned to each track i in an event hemisphere: ω_i is calculated from the track's impact parameter significances with respect to the primary and the secondary vertices. The B direction is calculated from the weighted sum of the track momenta $\sum_i \omega_i \cdot \vec{p_i}$ and from the primary to secondary vertex direction. A similar approach is used to determine the B energy assuming a two-body decay of the Z^0. The B* signal observed by OPAL using the full LEP1 data set is presented in Figure 1. A narrow peak on top of a smooth background yields 1894 ± 89 signal entries. The total efficiency for the reconstruction of converted photons from B* decays is 1.41% as calculated from Monte Carlo while the conversion probability in the inner tracking system is about 8%. The background stems mainly from true conversions from π^0. The results for the mass splitting and the production rate are [9]:

$$\Delta M(\mathrm{B}^*{-}\mathrm{B}) = (46.2 \pm 0.3_{\mathrm{stat}} \pm 0.8_{\mathrm{sys}})\ \mathrm{MeV} \qquad \frac{\sigma_{\mathrm{B}^*}}{\sigma_{\mathrm{B}} + \sigma_{\mathrm{B}^*}} = 0.76 \pm 0.04_{\mathrm{stat}} \pm 0.08_{\mathrm{sys}}\ .$$

The main systematic error on the mass splitting is obtained from a data/Monte Carlo comparison of π^0 signals with converted photons. For the production rate the dominant error comes from uncertainties in the shape of the helicity angular distribution. The OPAL results are in good agreement with other measurements (see Figure 2). The B* production rate is consistent with the naive spin counting prediction of 0.75. From a fit to the $\cos\theta^*$ distribution the fraction of the longitudinally polarised B* is measured to be $\frac{\sigma_l}{\sigma_l+\sigma_t} = 0.36 \pm 0.06_{\mathrm{stat}} \pm 0.07_{\mathrm{sys}}$, indicating an equal population of the longitudinal and transverse polarisation states. All results average over B^0, B$^\pm$ and B$^0_\mathrm{s}$ mesons.

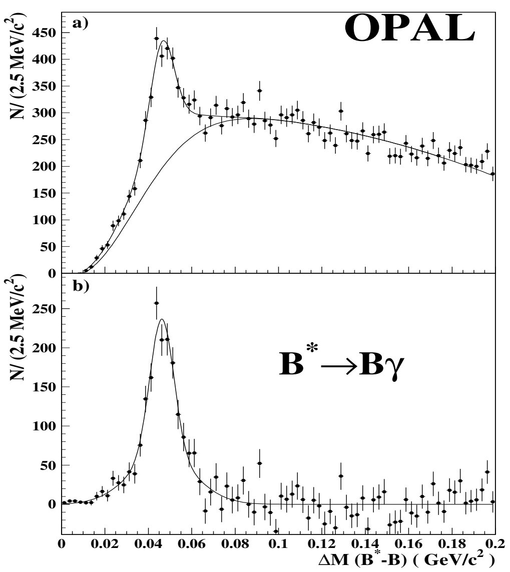

Figure 1. B* signal using $\gamma \to \mathrm{e}^+\mathrm{e}^-$.

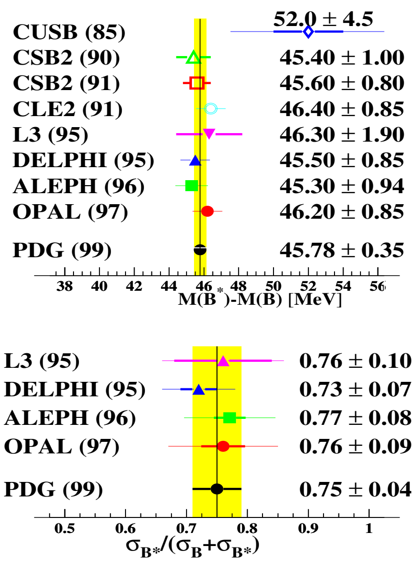

Figure 2. Comparison of B* results.

1.3. B_J^* **and** B_{sJ}^* **mesons**

B_J^* mesons are reconstructed by combining charged pions emerging from the primary vertex with B mesons. The B meson reconstruction is based on the method presented in Section 1.2. An estimation of the secondary vertex charge $q_{\mathrm{vtx}} = \sum_i \omega_i q_i$ using all charged tracks in a jet allows to define samples of unlike-sign ($\mathrm{B}^+\pi^-$) and like-sign ($\mathrm{B}^+\pi^+$) combinations[2]. The B_J^* signal (Figure 3a) is obtained by subtracting the invariant $\mathrm{B}\pi$ mass distribution of the like-sign sample from the corresponding distribution of the unlike-sign sample and by applying corrections to account for neutral B mesons misidentified as B^+ and for non-resonant $\mathrm{B}^+\pi^-$ combinations. This procedure provides a determination of the large combinatorial background largely independent from the simulation. The shape of the observed peak and a mass resolution of about 35 MeV suggests a superposition of several states, as expected from HQS. The signal of 1738 ± 121 candidates can be interpreted as

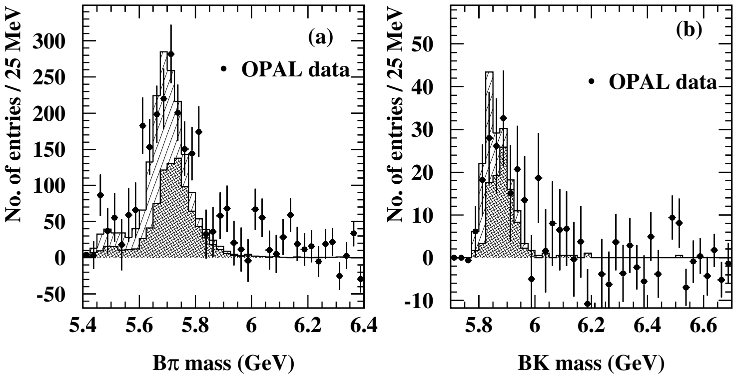

Figure 3. The B_J^* and B_{sJ}^* signals. The solid (hatched) histograms indicate possible $\mathrm{B}_{(s)2}^*$ ($\mathrm{B}_{(s)1}$) contributions.

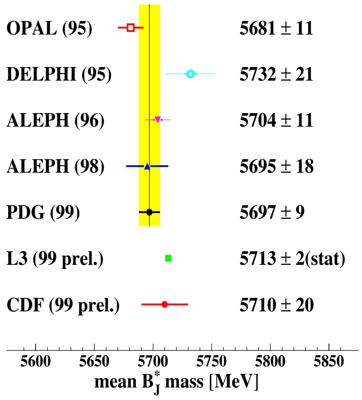

Figure 4. Comparison of different B_J^* mass measurements.

the sum of the decays $\mathrm{B}_2^* \to \mathrm{B}^{(*)}\pi$ and $\mathrm{B}_1 \to \mathrm{B}^*\pi$ represented in Figure 3a by the solid and shaded histograms respectively. Also broad B_J^* states (S-wave, see Figure 5) might contribute to the total signal. Replacing the π^- by a K^- and adjusting the selection cuts to the different kinematics, the B_{sJ}^* signal of Figure 3b is derived. From the $\mathrm{B}\pi$ and BK signals of Figure 3 the average mass of the B_J^* and B_{sJ}^* states (without any correction applied for decays to B^*) and the $\mathrm{B}_{(s)J}^*$ production rates per $\bar{\mathrm{b}}$ quark are obtained[3] [6]:

$$\langle M(\mathrm{B}_J^*)\rangle = (5681 \pm 11)\ \mathrm{MeV} \qquad \mathrm{f}(\bar{\mathrm{b}} \to \mathrm{B}_J^*) = 0.214 \pm 0.044 \qquad \text{(a)}$$
$$\langle M(\mathrm{B}_{sJ}^*)\rangle = (5853 \pm 15)\ \mathrm{MeV} \qquad \mathrm{f}(\bar{\mathrm{b}} \to \mathrm{B}_{sJ}^*) = 0.0199 \pm 0.0060 \qquad \text{(b)}$$

Both mass measurements are in good agreement with models [10] and the B_J^* mass is consistent with similar measurements (Figure 4). The observed B_{sJ}^* signal differs from a preliminary DELPHI result [11]. The measured B_J^* production rate is in agreement with other LEP results [3,4,7,8] while theoretical calculations [12] predict a somewhat higher B_J^* rate, depending on the fraction of narrow B_J^*. The distribution of the helicity angle of the pion in the $\mathrm{B}\pi$ rest-frame relative to the direction of flight of the $\mathrm{B}\pi$ system in the lab frame for entries in the signal region in Figure 3a is consistent with being isotropic.

[2] Charge conjugate processes are implied in this section.

[3] For the production rate calculation, I use the $\mathrm{B}^+/\mathrm{B}^0/\mathrm{B}_s^0/\mathrm{b}-$baryon admixture of [1].

1.4. Separation of $B_J^* \to B^*\pi^\pm$ and $B_J^* \to B\pi^\pm$ decays

Additional information is needed to resolve any B_J^* multiplet structure. As indicated in Figure 5, spin-parity conservation places restrictions on the dominant $B_J^* \to B^{(*)}\pi$ decay modes. Whereas a fit to the total $B\pi$ mass spectrum requires many additional assumptions inferred from theoretical considerations [3], a separation of the $B_J^* \to B^*\pi^\pm$ and $B_J^* \to B\pi^\pm$ decay modes is a natural step towards a better understanding of the B_J^* signal based solely on experimental observations. A direct reconstruction of the $B\gamma\pi$ final state suffers from high backgrounds and moderate mass resolution and is therefore not feasible. The OPAL analysis, tuned to high efficiencies, uses improved B and B^* reconstruction methods yielding more than 75 000 $B^* \to B\gamma$ candidates which are used to calculate the probability

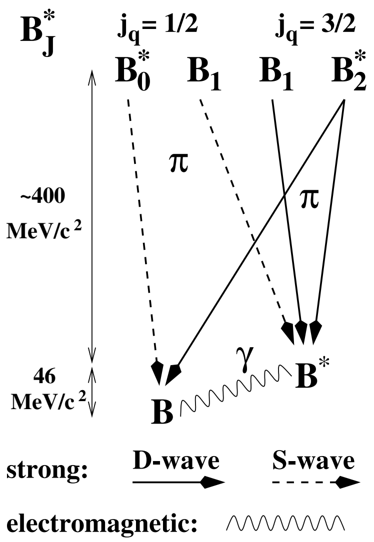

Figure 5. B_J^* multiplet.

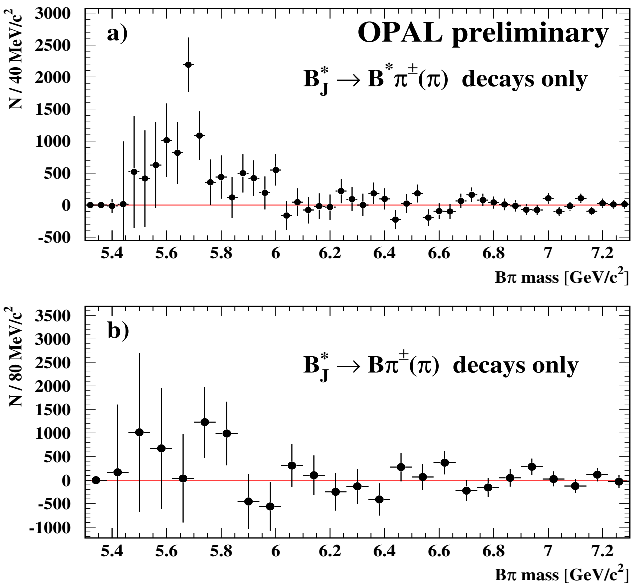

Figure 6. $B_J^* \to B^*\pi^\pm$ and $B_J^* \to B\pi^\pm$ decays.

$\mathcal{W}(B^*)$ for each B candidate to have come from a true B^*. B_J^* candidates are reconstructed in the $B\pi^\pm$ channel. With a cut on $\mathcal{W}(B^*)$ the total sample of B_J^* candidates is divided into two mutually exclusive samples enriched and depleted in the decay $B_J^* \to B^*\pi^\pm$. From the number of $B\pi^\pm$ candidates observed in the B^*-enriched and B^*-depleted signals the branching ratio of orbitally excited B mesons decaying to B^* is measured [13]:

$$\mathrm{BR}(B_J^* \to B^*\pi) = 0.85\,^{+\,0.26}_{-\,0.27\,\mathrm{stat}} \pm 0.12_{\mathrm{sys}}$$

For the determination of the combinatorial $B\pi$ background a new method described in [13] is used. The dominant error sources are the sideband normalisation and the photon reconstruction efficiencies, but not the $B\pi$ background shape. The result is in agreement with the measured B^* and B_J^* production rates at LEP. From a linear combination of the efficiency-corrected $B\pi^\pm$ signals of the B^*-enriched and B^*-depleted samples the $B\pi$ mass spectra of pure $B_J^* \to B^*\pi^\pm$ and $B_J^* \to B\pi^\pm$ decays are derived (Figure 6). A clear signal for $B_J^* \to B^*\pi^\pm$ decays is observed for the first time (Figure 6a), whereas the excess of entries in the $B_J^* \to B\pi^\pm$ mass spectrum is not significant (Figure 6b).

2. A SEARCH FOR THE TENSOR GLUEBALL

2.1. Motivation

Lattice QCD calculations provide quite accurate predictions for the mass spectrum of pure gluonic states below 3 GeV. For the $J^{\mathrm{PC}} = 2^{++}$ state, masses around 2.2 GeV have been calculated [14]. Since the first experimental evidence for a narrow state in this mass region [15] many measurements with sometimes conflicting results have been reported [1]. Recently the L3 collaboration claimed preliminary evidence for $\mathrm{f}_J(2220) \rightarrow \mathrm{K^0_sK^0_s}$ production in hadronic Z^0 decays [16]. This result caused lively interest since in this analysis the $\mathrm{f}_J(2220)$ signal is mainly seen in the lowest-energetic jet of three-jet events. Therefore a similar analysis has been performed by the OPAL collaboration [17].

2.2. The OPAL analysis

For the reconstruction of $\mathrm{f}_J(2220)$ candidates, the whole LEP1 data set of about $4.3 \cdot 10^6$ $\mathrm{Z}^0 \rightarrow \mathrm{q\overline{q}}$ decays, recorded with the OPAL detector, is used. $\mathrm{K^0_s}$ candidates are reconstructed in the dominant $\pi^+\pi^-$ final state. The OPAL tracking system is well-suited for this task, since the large jet chamber with an outer radius of 1.8 m provides a high acceptance for the reconstruction of long-lived particles over a large momentum range. A kinematic and geometric fit is performed on the decay tracks of the selected $\mathrm{K^0_s}$ to improve the $\mathrm{K^0_s}$ momentum resolution. $\mathrm{K^0_s}$ are then combined into pairs to form $\mathrm{f}_J(2220)$ candidates. Monte Carlo studies simulating a narrow $\mathrm{f}_J(2220)$ with mass and width according to [1] indicate a $\mathrm{f}_J(2220)$ mass resolution of about 12 MeV. The purity of the $\mathrm{K^0_s}$ sample is approximately 80% and the reconstruction efficiency for $\mathrm{f}_J(2220)$ is about 11%. The simulation shows that the efficiency is roughly independent of the $\mathrm{f}_J(2220)$ energy and distribution of the helicity angle. The sensitivity to the $\mathrm{f}_J(2220)$ signal is higher than the sensitivity of the L3 analysis [16]. The $\mathrm{K^0_sK^0_s}$ invariant mass spectrum of all $\mathrm{f}_J(2220)$ candidates is shown on the left side of Figure 7. No signal is observed while a narrow peak is expected for $\mathrm{f}_J(2220)$ from the simulation (shaded histogram). In the absence of a signal, an upper limit on the production rate of $\mathrm{f}_J(2220)$ times the branching ratio into $\mathrm{K\bar{K}}$ in hadronic Z^0 decays is calculated:

$$\mathrm{n}_{\mathrm{f}_J(2220)} \cdot \mathrm{BR}(\mathrm{f}_J(2220) \rightarrow \mathrm{K\bar{K}}) < 0.0028 \qquad @\ 95\%\mathrm{C.L.}$$

For this limit, a width of $\Gamma(\mathrm{f}_J(2220)) = 23$ MeV [1] has been assumed. The limit is dominated by the statistical error and the 95% exclusion line is shown in Figure 7.

Any differences of glueball production in quark and in gluon jets are investigated by forcing each event to a three-jet topology using the Durham jet-finder with a y_{cut} of 0.005. Then $\mathrm{f}_J(2220)$ candidates are formed from pairs of $\mathrm{K^0_s}$ assigned to the same jet only. The jets are ordered according to decreasing jet energies. The Monte Carlo indicates that about 75% of the lowest-energetic jets can be associated with primary gluons. The $\mathrm{K^0_sK^0_s}$ mass spectrum for the gluon-enriched jet sample is shown on the right side of Figure 7. Again, no signal is observed. An upper limit (using the dominant statistical error only) on the number of $\mathrm{f}_J(2220)$ seen in the gluon-enriched sample yields :

$$\mathrm{N}(\mathrm{f}_J(2220) \rightarrow \mathrm{K^0_sK^0_s} \rightarrow 2(\pi^+\pi^-)) < 8.3 \text{ events} \qquad @\ 95\%\mathrm{C.L.}$$

Translating the corresponding L3 result [16] to the higher selection efficiency of the OPAL analysis one obtains an expectation of 89 ± 17 signal events. Thus the evidence for $\mathrm{f}_J(2220)$

production by the L3 collaboration is not confirmed by the similar OPAL analysis. Results from other LEP experiments are desirable to clarify the observed discrepancy in $f_J(2220)$ production in $Z^0 \to q\overline{q}$ decays.

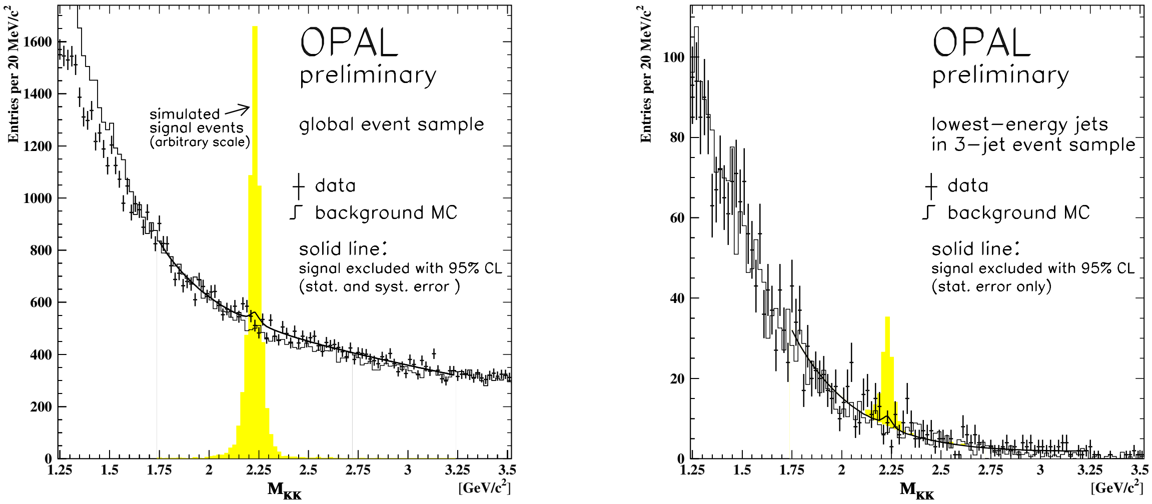

Figure 7. $K_s^0K_s^0$ mass spectra of the global event sample and the gluon-enriched sample.

ACKNOWLEDGEMENTS

I would like to thank the organisers of this interesting conference for the invitation to present OPAL spectroscopy results. I am grateful to many of my colleagues on OPAL, especially Thomas Kress for the fruitful discussions on glueballs.

REFERENCES

1. Particle Data Group, C. Caso et al., Eur. Phys. J. C3 (1998) 1.
2. For example: F. Ledroit (for the DELPHI collaboration), Nucl. Phys. B Proc. Suppl. 64 (1998) 411.
3. L3 collaboration, M. Acciarri et al., CERN-EP-99-116, submitted to Phys. Lett. B.
4. ALEPH collaboration, R. Barate et al., Phys. Lett. B425 (1998) 215.
5. G. Bauer (for the CDF collaboration), FERMILAB-Conf-99/227-E, hep-ex/9909014.
6. OPAL collaboration, G. Alexander et al., Z. Phys. C66 (1995) 19.
7. DELPHI collaboration, P. Abreu et al., Phys. Lett. B345 (1995) 598.
8. ALEPH collaboration, D. Buskulic et al., Z. Phys. C69 (1996) 393.
9. OPAL collaboration, K. Ackerstaff et al., Z. Phys. C74 (1997) 413.
10. For example: D. Ebert, V.O. Galkin, R.N. Faustov, Phys. Rev. D57 (1998) 5663; *Erratum* ibid. D59 (1999) 019902.
11. DELPHI collaboration, contributed paper eps0563 to HEP95 Brussels, DELPHI-95-105.
12. Yi-Jin Pei, Z. Phys. C72 (1996) 39.
13. OPAL collaboration, contributed paper to HEP99 Tampere and Hadron99 Beijing, OPAL Physics Note PN400 (1999).
14. For example: UKQCD collaboration, G. Bali et al., Phys. Lett. B309 (1993) 378.
15. MARK III collaboration, R. M. Baltrusaitis et al., Phys. Rev. Lett. 56 (1986) 107.
16. G. Forconi (for the L3 collaboration), *Indication of* $\xi(2230)$ *Production in Hadronic* Z^0 *Decays*, Proceedings of the 7$^{\text{th}}$ Int. Conference on Hadron Spectroscopy (1997) 737.
17. OPAL collaboration, contributed paper to HEP99 Tampere, OPAL Physics Note PN357 (1998).